PAPER

Fluorescence lifetime imaging reveals heterogeneous functional distribution of eGFP expressed in *Xenopus* oocytes

Methods and Applications in Fluorescence

PAPER

Fluorescence lifetime imaging reveals heterogeneous functional distribution of eGFP expressed in *Xenopus* oocytes

Steven L Zeng, Dorota Grabowska, Kiana Shahverdi, Leland C Sudlow, Samuel Achilefu and Mikhail Y Berezin

Department of Radiology, Washington University School of Medicine, St. Louis, MO 63110, United States of America

E-mail: berezinm@wustl.edu

RECEIVED
7 June 2019

REVISED
6 September 2019

ACCEPTED FOR PUBLICATION
28 October 2019

PUBLISHED
13 November 2019

Keywords: *Xenopus* oocytes, fluorescence lifetime, eGFP, oocyte polarity

Abstract

The oocytes from *Xenopus laevis* are well known for their polarity, presenting a distinct animal and vegetal pole. Other heterogeneities are less known. To study the heterogeneity of the *Xenopus* oocyte, we expressed eGFP and analyzed the protein distribution with fluorescence lifetime microscopy. The vegetal pole exhibited higher levels of fluorescence, than the animal pole. However, the fluorescence lifetimes between the two areas were indistinguishable, suggesting similar environments. In contrast, we observed a substantial and gradual decrease in the fluorescence lifetime from 2.9 ns to 2.6 ns as slices approached the periphery. This has an important implication for future oocyte studies as it demonstrates the environment inside the oocyte is not uniform and might affect the fluorescence intensity. As a result, it cannot be assumed that the observed fluorescence intensity reflects the expression of the proteins but might reflect the environment within the oocyte.

Introduction

The African clawed frog (*Xenopus* laevis) is essential to many developmental, differential, and embryological studies in vertebrates. Their oocytes are important and unique cell model in biomedical research, especially in the field of electrophysiology [1], studying ion channels [2], and drug discovery [3]. One of the key features of *Xenopus* oocytes is their ability to express nearly any exogenous protein from a large variety of species within 48 h with with a very high success rate [4], making them excellent models of disease. Physical robustness and tolerance to a range of physical manipulations such as dissections, injections, and transplantations make oocytes a system of choice in a wide range of fields, including developmental biology [5], cardiology [6], neurological diseases [7], and general cell and molecular biology [8]. The oocyte's expression system is particularly suitable to electrophysiological studies because of the large size (1.2 mm in diameter) of the oocyte and spherical shape, facilitating the insertion of electrodes and adequate voltage control [9]. In addition, each oocyte provides a fairly substantial quantity of material for a biochemical assay, enabling microscopy studies on different cross-sections and analyzing spatial distribution of the molecule such as expressed proteins.

In contrast to conventional cells, the unfertilized *Xenopus* oocytes are not unidirectional and have a strong degree of polarity. This polarity reflects that the maternal factors stored in the form of RNAs and proteins has a polarized distribution along the animal–vegetal (A–V) axis within the oocyte cytoplasm [10]. In addition, the polarity of the *Xenopus* oocyte also affects many cellular components. This heterogeneity extends deeper than the cell membrane of the oocyte and affects the distribution of the mitochondria, ribosomes, cytoplasm, and yolk platelets [11, 12]. A prominent feature of oocytes is the presence of drastically different animal and vegetal poles (figure 1). These poles can be determined by the striking black and white colored hemispheres of the oocyte with the darker region representing the animal pole and the lighter containing the vegetal pole.

The heterogeneous distribution of proteins and organelles in *Xenopus* oocytes can have major effects on experimental design. This is particularly relevant for research involving membrane transport proteins as many studies reference a clear difference in channel or receptor density between the animal and vegetal

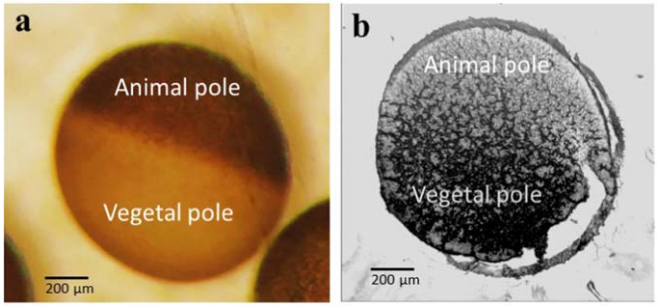

Figure 1. Brightfield microscopy of *Xenopus* oocytes showing animal and vegetal poles. Animal poles were oriented at the top of each image. (a) Exterior of *Xenopus* oocyte shows a distinct black and white coloration, which matches the internal distribution of yolk platelets. (b) section of *Xenopus* oocyte imaged under light microscopy shows evidence of a heterogeneous distribution of yolk platelet density within the oocyte.

poles [13, 14]. This variance in receptor density guides many aspects of electrophysiological experiments, including how the oocyte is positioned and where on the membrane the experiment is performed. Despite this, previous studies have rarely gone beyond citing a difference in expression and often overlooked if cellular localization has an effect on protein function as well.

To investigate whether the heterogeneous distribution of proteins affects their functional expression we transfected an oocyte with a plasmid carrying an enhanced green fluorescent protein (eGFP). eGFP [15] is a relatively small protein (27 kDa) that is like its predecessor GFP and other fluorescent proteins that are frequently used in oocytes as a fusion protein to report the spatial distribution of the protein of interest [16, 17]. The small size of eGFP does not affect the intended function of other proteins and, in general, does not interfere with the protein localization within the cell. However, the fluorescence from green fluorescent proteins is typically affected by a number of intercellular environmental factors such as pH [18], intercellular viscosity [19] and oxygenation level [20]. Conventional fluorescence microscopy is unable to distinguish these factors since the generated fluorescence intensity image only provides the location, which can lead to incorrect conclusions.

To address this question, we present a method that integrates fluorescence intensity images with the fluorescence lifetime microscopy (FLIM) of oocytes expressing fluorescent proteins. The advantage of FLIM imaging methodology lies in its independence on concentration and how it only reflects the environment around the fluorophore [21, 22]. Thus while conventional fluorescence intensity based microscopy can only determine the spatial location of GFP, FLIM provides additional information on the functional status. To the best of our knowledge this is the first study that addresses the spatial characterization of GFP in oocytes using FLIM.

Experimental methods

cDNA preparation

pUNIV-EGFP [23] was a gift from Cynthia Czajkowski (Addgene plasmid #24706; http://n2t.net/addgene:24706; RRID:Addgene_24706) and was received from Addgene as a bacterial stab. *Escherichia coli*, containing the plasmids, were re-plated on nutrient agar plates with ampicillin and grown at 37 °C overnight. After 12 to 18 h the single colonies were transferred into 4 ml of previously frozen liquid broth medium containing ampicillin (final conc. of ampicillin is 100 μg ml^{-1}) in a 4 ml cell culture tube. The cultures were then incubated overnight at 37 °C under constant steady shaking at 225 rpm. After shaking, the bacterial colonies were collected and the plasmids were isolated from the bacterial cells using Qiagen Spin Miniprep Kit (Qiagen). The plasmid were stored on ice (4 °C) for several days prior the injections into the oocytes. The final concentration of eGFP containing cDNA was measured with Nanodrop (ThermoFisher) and was found to be 606 ng μl^{-1}.

Expression in *Xenopus* oocytes

Defolliculated stage V and VI oocytes (diameter ~1.2 mm) from *Xenopus laevis* were obtained from Ecocyte Bioscience in April—May 2019 and stored in ND96 saline (NaCl 96 mM, KCl 20 mM, $CaCl_2.2H_20$ 1.8 mM, $MgCl_2.6H_20$ 1 mM, HEPES 5 mM, pH 7.6) supplemented with sodium pyruvate (2.5 mM) and 1 ml/100 ml penicillin-streptomycin (10,000 units penicillin, 10 mg/ml streptomycin). Storage media were changed daily, and oocytes were stored at 17 °C. The oocytes were injected with 18 nL of eGFP cDNA (200 μg ml^{-1}) using a Nanoliter 2010 micro-injector (World Precision Instruments). Injection micropipettes were pulled on a Sutter Instrument Model P-1000, using fire polished glass capillaries (ID = 0.530 mm, OD = 1.14 mm). Prior to injection, the oocytes were aligned with the animal pole facing upward, and the injection needle was positioned for best approximation for direct nuclear injection. Following injection, oocytes were returned to ND96

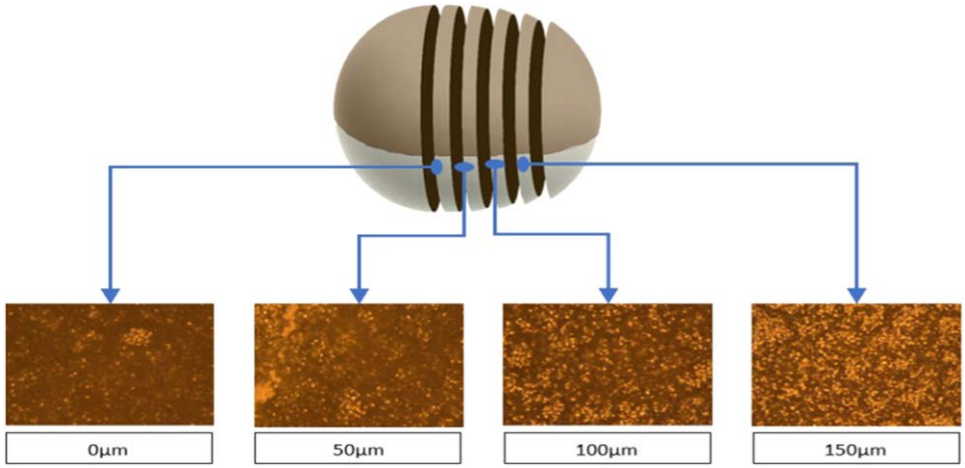

Figure 2. Images of *Xenopus* oocyte cytoplasm near the apex of the vegetal pole. Images were collected under standard light microscopy with the darker regions representing the dense yolk platelets. Apex of the vegetal pole is towards the bottom of the oocyte model. Slices (25 μm thick) were collected in 50 μm intervals from the vertical midline of the oocyte. Arrows indicate approximate location within the cell where the slices were collected.

saline for incubation for 48 h at 17 °C and then dissected by cryo-sectioning.

Cryo-sectioning of oocytes and tissue preparation

After 48 h following cDNA injection, oocytes were placed in disposable plastic embedding molds and the molds were filled with OCT (Sakura Finetek). Samples were frozen using dry ice and stored at −80 °C. Frozen samples were sectioned into 25 μm thick slices using a Kryostat 1720 (Leica). The slices were made with 50 micron splicing between the slices to prevent tear (figure 2). The sections were mounted on Colorview Adhesion Slides (StatLab) and immersed in a 50:50 (%) ethanol-methanol solution for fixation.

Fluorescence imaging

Oocyte sections were placed on a glass slide, covered with a coverslip, and imaged under an Olympus BX51WI microscope, equipped with a metal halide light source (X-cite), an emission/excitation FITC 5058A-OMF filtercube (Semrock) and objective EC Plan-Neofluar 5×(Zeiss). Fluorescence intensity images were collected using a cooled CCD camera ORCA-ER (Hamamatsu). The images were analyzed using ImageJ.

Fluorescence lifetime imaging

Fluorescence lifetime imaging microscopy (FLIM) was performed on a MicroTime 200 time-resolved confocal laser scanning fluorescence microscope (PicoQuant) based on an inverted microscope (IX 71, Olympus) equipped with an Olympus PlanN 40× objective. The FLIM system undergoes self-calibration after it turned on. Overall calibration of the system was judged by the instrument response function per the manufacturer guideline. The sample was excited using 485 nm pulsed laser and emission fluorescence was collected with a 519 nm long pass emission filter. Time-resolved images were analyzed with the SymphoTime software (PicoQuant). Collected decay data and the instrument response function (IRF) were fit to exponential decay equations using n-exponential method. Most of the fits were based on a single exponential decay according to the equation (1). Such fits provided an acceptable level of χ^2 values (within the range 1.1 to 1.3).

$$y(t) = Ae^{-t/\tau}$$

(eq 1)Where τ is the fluorescence lifetime, A is the amplitude of the signal, t decay time.

Statistical testing

Data were tested either via an unpaired t-test or ANOVA with Tukey's multiple comparisons test. Results were considered significantly different at $p < 0.05$. Error was determined using standard error of mean.

Results and discussion

Oocyte cytoplasm demonstrates heterogeneous environment

The subcellular localization of a genetically encoded protein is often tied to its function, so it is imperative to determine where the protein of interest resides [24]. There are a variety of methods for determining the spatial expression of proteins. One of the most general approaches is to identify the localization of the expressed protein of interest with a protein-specific fluorescently labeled antibody. Another common approach is to fuse a protein with fluorescent fusion proteins [25]. Both methods rely on fluorescence microscopy to quickly and reliably identify the location of the protein. By examining the spatial distribution of fluorescent signal in the cell with fluorescence

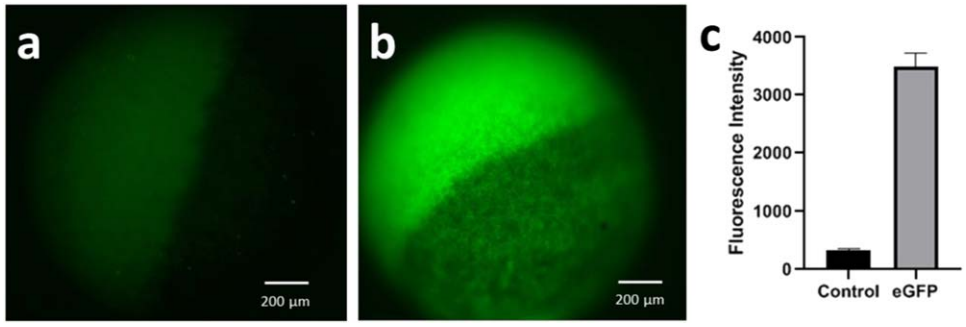

Figure 3. Fluorescence in intact oocytes (a) control, no plasmid added (autofluorescence), (b) 48 h after pUNIV-EGFP after the transfection, (c) emission signals intensity in the vegetal pole of the oocytes. FITC filtercube, objective 5×.

microscopy, one can assess where the protein in the cell is located.

However, fluorescence intensity images have several caveats. First, the intensity of the expressed fluorescence often depends on the environmental factors within the cell such as pH [26–28], intercellular viscosity [19], oxygenation levels [20], as well as aggregation. Second, which is relevant to oocytes, fluorescence signal can be hindered by the presence of light-blocking or light-absorbing components such as melanin. Thus, verifying the localization of the protein just from the fluorescence intensity alone is insufficient and might lead to erroneous conclusions. There is a need of another, concentration independent technique, such as FLIM, to confirm that the expressed protein targeted to various subcellular structures are equally functional.

In frog oocytes (figure 1), the animal hemisphere is dark brown, and the vegetal hemisphere is only weakly pigmented with a marginal, poorly pigmented zone in between (figure 1(a)). This visible polarity is quite unique for frog oocytes and has a major influence on the emergence of the embryonic structures as well as being responsible for the future appearance of different organs [29]. The polarity also implies a directional transport of mRNAs, including that of the transcribed foreign proteins.

To examine how the oocyte's polarity affects protein expression and distribution, we transfected the oocytes with the eGFP containing vector pUNIV-EGFP developed for the transfection of oocytes as well as mammalian cells [23]. Successful expression of eGFP in *Xenopus* oocytes 48 h after the injection was confirmed via fluorescence microscopy (figure 3). Fluorescence signal from the eGFP-expressed oocyte was more than 10 times stronger than from the untreated, control oocyte. The residual fluorescence seen in the untreated oocytes was likely to be due to autofluorescence, and is considered to be negligible under the applied excitation–emission conditions [30].

Forty-eight hours post-transfection, the oocyte was cryo-sectioned over a range of distances from the periphery towards the center of the cell. Starting from the periphery, we collected slices at 50 μm intervals until reaching the vertical midline on the A-V axis. We observed that the oocyte sections often tore from the slicing procedure. Sections closest to the periphery were significantly damaged and were consequently, discarded. Under brightfield microscopy, we identified an internal division in the density of yolk platelets with the vegetal pole containing more densely packed yolk platelets than the animal pole as seen by the darker coloration (figure 1(b)). This sharp division in platelet density corresponded with the division in the outer plasma membrane pigmentation.

In addition to the variation in platelet density within individual oocyte sections, we also observed a yolk platelet density gradient between sections. Slices collected closer to the vertical midline of the oocyte had a higher concentration of darker, dense yolk platelets in the vegetal pole when compared to more peripheral slices of the vegetal pole. This gradient in yolk platelet density was also observed in the animal pole to a lesser degree.

Fluorescence microscopy shows heterogeneous distribution of eGFP

Next, we analyzed the fluorescence intensity maps from each oocyte section. An example of such imaging is shown in figures 4(a)–(c). Similar to the images collected under the brightfield condition, the fluorescent images revealed a heterogeneous distribution within the cytoplasm with the vegetal pole shower significantly higher levels of fluorescence intensity (figure 4(d)). In addition, we observed the radial distribution of the fluorescence intensity: the average fluorescence of each oocyte section increased with their proximity to the center of the cell (figure 4(e))

Fluorescence lifetimes of cytosolic eGFP

Due to the technical limitations, the FLIM system can only image a relatively small field of view (ca. 100 × 100 micron) with the 40× objective (working distance 0.6 mm). For this reason, we captured fluorescence lifetime images from several areas in cytoplasm in the vegetal and animal poles. The examples of the lifetime images are shown in

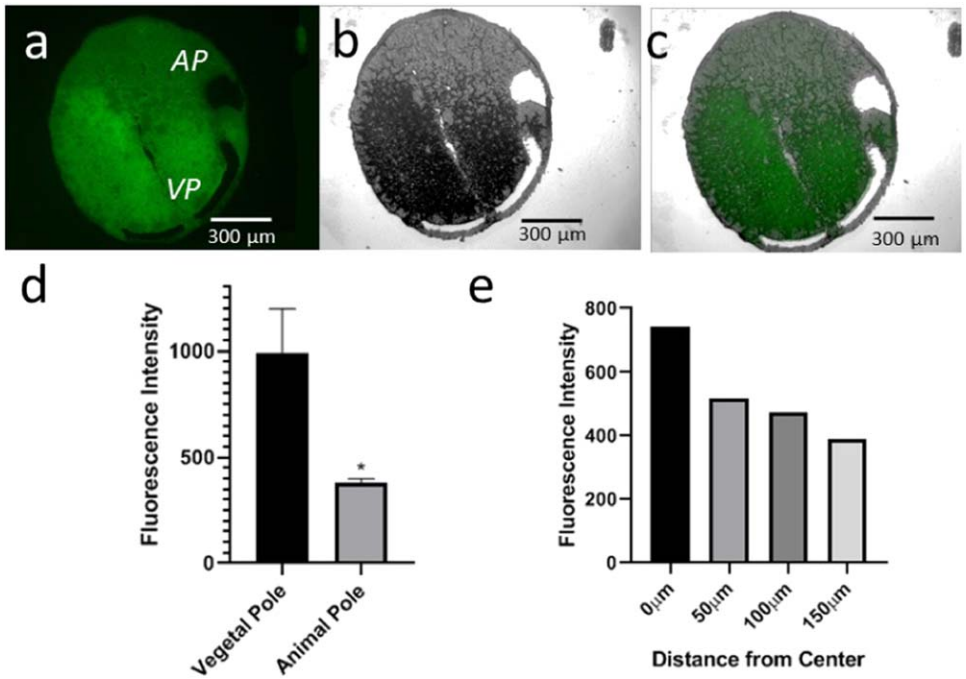

Figure 4. Fluorescent microscopy of oocytes sections with expressed eGFP from the vegetal (VP) and animal poles (AP). Images of *Xenopus* oocyte slices are positioned with animal pole at the top and the fluorescence intensity was measured. (a) Fluorescence microscopy image of *Xenopus* oocyte slice expressing GFP. (b) Standard light microscopy image of *Xenopus* oocyte slice. (c) Overlay of fluorescence and light microscopy images of *Xenopus* oocyte slices. (d) Comparison of fluorescence intensity between cytosolic regions from the vegetal and animal poles ($n = 4$). Fluorescence intensity was measured from the entire vegetal or animal pole region. Significance was determined using an unpaired t-test with a $P < 0.05$. (e) Comparison of fluorescence intensity from sections of *Xenopus* oocyte taken from varying slices of the cell. Each column represents the average fluorescent value of a single cross-section.

figures 5(a), (b), the average lifetime calculated (figure 6(a)).

We found that there was no significant difference in the fluorescence lifetime between the fluorophores located near the vegetal and animal poles within each slice (figure 6(a)). Both poles show an average fluorescence lifetime of 2.7 ns, which is similar to the range that has been reported for eGFP [31]. These values are likely to reflect only the fluorescence from the expressed eGFP. Due to the low autofluorescence intensity, fluorescence the lifetimes from the control untreated oocytes were difficult to measure: the decays were mostly undistinguishable from the instrument response functions.

These data suggests that eGFPs in both poles are functionally similar and that the observed difference in the fluorescence intensity shown in figure 4 is due to the difference in the expression level of eGFP.

Curiously, we identified a gradient of the fluorescence lifetime of the eGFP inside the oocyte. Using oocyte slices collected in 50 μm intervals from the vertical midline of the cell, we found a downward trend in fluorescence lifetime with slices further away from the center having shorter lifetimes (figure 6(b)). This trend was the same in both poles.

From the measurements of fluorescence intensity, we have observed a consistent phenomenon that there is increased fluorescence localized in the vegetal pole of the *Xenopus* oocyte as well as in the center of the oocyte (figure 5). This non-uniform distribution of fluorescence could be the result of several factors. These include a simple heterogeneity in the spatial distribution within the cytosol, with the animal pole having a lower concentration of proteins and the regions closest to the vertical midline having the highest fluorescence intensity. Additionally, it could be the result of a dampening or quenching of the fluorophore based on changes in environment between the animal and vegetal pole and between the center and periphery of the cell.

To shed light on this, we employed fluorescence lifetime imaging as a well-known tool to examine the functional differences between the fluorophores from different regions of the oocyte. To do so, we sectioned the oocyte to remove some potential artifacts associated with the depth of the fluorescence signal. Based on the results shown in figures 5 and 6(a). We found that there was no significant difference in the lifetime between regions in the animal and vegetal poles within the same oocyte slice. This was consistent for all slices collected. However, as the slices moved closer to the periphery of the oocyte, there was an apparent decrease in the fluorescence lifetime, indicating a change in environment between the center and edges of the oocyte. As a result, the downward shift in intensity towards the edges of the oocyte cannot be entirely explained by an uneven spatial distribution and may by the result of a different environment such as pH,

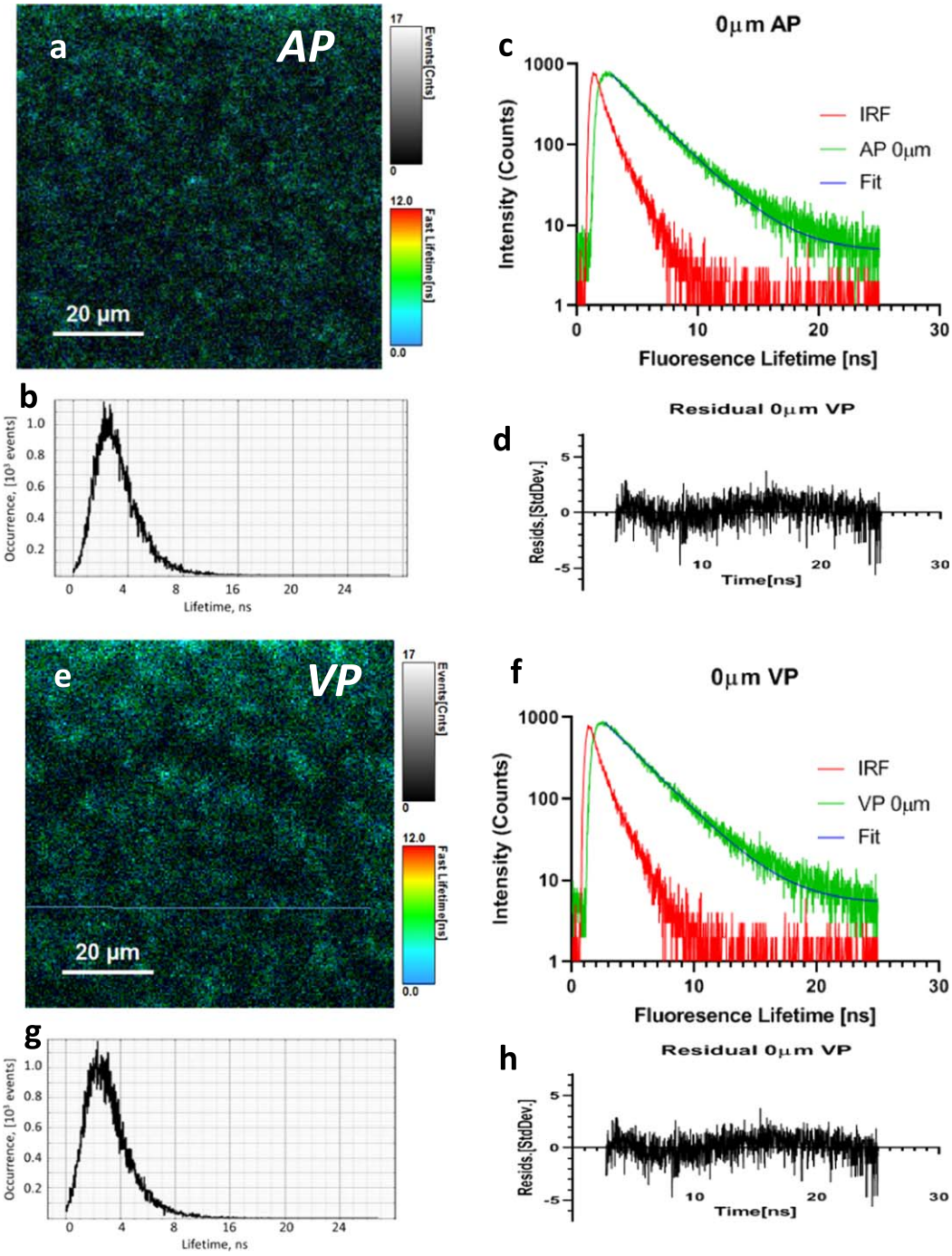

Figure 5. Fluorescence lifetime images of eGFP expressed *Xenopus* oocyte cytoplasm and their corresponding lifetime distribution. (a)–(d) Fluorescence lifetime of the animal pole of cytoplasm from the apex of *Xenopus* oocyte slice, lifetime distribution, decays, residual, ($\tau = 2.87$ ns, single exponentional fit, $\chi^2 = 1.18$). Brighter regions indicate areas of fluorescence. (e-h) Fluorescent lifetime of the vegetal pole of cytoplasm from the apex of *Xenopus* oocyte slice, lifetime distribution, decays, residual, ($\tau = 2.87$ ns, single exponentional fit, $\chi^2 = 1.19$).

viscosity [32], differences in refractive index [33, 34] or presence of different ions, creating a quenching effect, as well as self-quenching due to the high level of eGFP expression. Similar to our results, it has been earlier observed in living human myeloid cells that GFP-labelled membrane proteins have a shorter lifetime than in the cytoplasm [35]. The gradient of the fluorescence lifetime has been also used to sense intracellular environment during the cell cycle of HeLa cells [36]. And the fact that fixed and live cells with GFP can have a different lifetime (depending on the mounting medium) can too be put down to explain the observed results [37, 38]. Understanding of these gradient lifetime phenomena in oocytes in greater details will be a focus of following studies and their potential applications to monitor different biological processes.

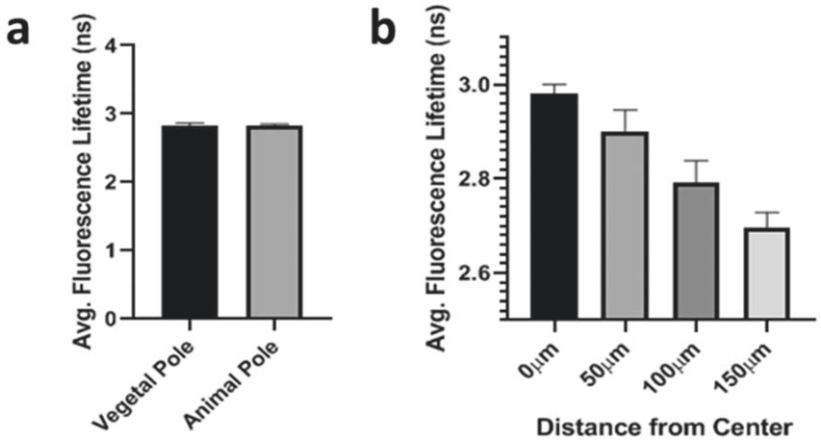

Figure 6. Fluorescence lifetime from eGFP expressed in *Xenopus* oocytes from multiple cross-sections. (a) Fluorescence lifetime of cytoplasm in the animal and vegetal poles shows no significant difference. Significance was determined using an unpaired *t*-test with a $p > 0.05$. (b) Comparison of fluorescence lifetime profiles of *Xenopus* oocyte slices taken from varying areas of the cell. Significance was determined using Tukey's multiple comparisons test with $p < 0.01$.

Conclusions

Using the fluorescence lifetime comparisons between vegetal and animal poles, we have confirmed that there is no functional difference in the eGFP expressed in each pole and that the difference in fluorescence intensity seen within individual slices is the result of an uneven distribution of protein expression. However, the fluorescence lifetime of the protein seems to be altered across the oocytes with an obvious trend of decreasing the lifetime from the center to the periphery of the oocyte. This finding contradicts the general belief that freely floating cytosolic proteins diffuse and distribute themselves evenly within oocytes and presents questions related to behavior of other cytosolic proteins in *Xenopus* oocytes. This has an important implication for future oocyte studies as it demonstrates the environment inside the oocyte is not uniform and might affect the fluorescence intensity. As a result, it cannot be assumed that the observed fluorescence intensity reflects the expression of the proteins but might reflect the environment within the oocyte. We suggest that future studies related to the expression of proteins in oocytes include fluorescence lifetime measurements whenever it's possible as a powerful and elegant method to evaluate the functional distribution of the fusion proteins carrying a fluorescent reporter. It is also possible to further understand the environmental change inside the oocyte. Such variations in the cytoplasmic milieu may play a critical role in the functioning of other transfected fusion proteins such as ion channels, receptors, and enzymes in the oocyte expression system. By using FLIM with specific fluorescent probes for key cytoplasmic ions, a better understanding of the interaction between the cytoplasm and expressed proteins can be gained. Given the importance of the oocytes in drug discovery, we believe that FLIM can greatly assist in the planning and interpretation of the results.

Acknowledgments

The authors thanks Washington University Optical Spectroscopy Core Facility (NIH 1S10RR031621), NIH R01CA208623 (MB), NSF 1827656 (MB), and S10OD016237 (SA). The authors have declared that no conflicting interests exist.

ORCID iDs

Mikhail Y Berezin https://orcid.org/0000-0002-2670-2487

References

[1] Stühmer W and Parekh A B 1995 Electrophysiological recordings from *Xenopus* oocytes *Single-channel recording* (Berlin: Springer) pp 341–56
[2] Dascal N 1987 The use of *Xenopus* oocytes for the study of ion channel *Critical Reviews in Biochemistry* **22** 317–87
[3] Kvist T, Hansen K B and Bräuner-Osborne H 2011 The use of *Xenopus* oocytes in drug screening *Expert Opin. Drug Discovery* **6** 141–53
[4] Delpire E, Gagnon K B, Ledford J J and Wallace J M 2011 Housing and husbandry of *Xenopus* laevis affect the quality of oocytes for heterologous expression studies *J. Am Assoc. Lab. Anim. Sci.* **50** 46–53
[5] Olsen R W and Tobin A J 1990 Molecular biology of GABAA receptors *The FASEB Journal* **4** 1469–80
[6] Zou A, Xu Q P and Sanguinetti M C 1998 A mutation in the pore region of HERG K + channels expressed in *Xenopus* oocytes reduces rectification by shifting the voltage dependence of inactivation *The Journal of Physiology* **509** 129–37
[7] Meisler M H and Kearney J A 2005 Sodium channel mutations in epilepsy and other neurological disorders *The Journal of Clinical Investigation* **115** 2010–7
[8] Dumont J N 1972 Oogenesis in *Xenopus* laevis (Daudin). I. Stages of oocyte development in laboratory maintained animals *J. Morphol.* **136** 153–79

[9] Bianchi L and Driscoll M 2006 Heterologous expression of C. elegans ion channels in *Xenopus* oocytes *WormBook: The Online Review of C. elegans Biology [Internet]* ed Martin Chalfie (On-line: WormBook) the On-line review of C-elegans biology (https://doi.org/10.1895/wormbook.1.7.1)
[10] Kloc M, Kloc M and Kubiak J Z 2014 Polarity of *Xenopus* oocytes and early embryos *Xenopus Development* (Hoboken, New Jersey, United States of America: John Wiley & Sons, Inc.) pp 424
[11] Danilchik M V and Gerhart J C 1987 Differention of the animal-vegetal axis in *Xenopus* laevis oocytes: I. Polarized intracellular translocation of platelets establishes the yolk gradient *Dev. Biol.* **122** 101–12
[12] Gordon R, Breward C, Cumberbatch E, F Williams J, Bohun S, Aruliah D A and Lewis G M 2006 Yolk dynamics in amphibian embryos *Fields–MITACS Industrial Problems Workshop* (Toronto, Ontario, Canada: The Fields Institute for Research in Mathematical Science)
[13] Maksaev G and Haswell E S 2015 Expressing and characterizing mechanosensitive channels in *Xenopus* oocytes *Plant Gravitropism* (*Methods in Molecular Biology* 1309) ed) ed Elison B. Blancaflor (New York: Springer) 151–69
[14] Machaca K and Hartzell H C 1998 Asymmetrical Distribution of Ca-Activated Cl Channels in *Xenopus* Oocytes *Biophys. J.* **74** 1286–95
[15] Cormack B P, Valdivia R H and Falkow S 1996 FACS-optimized mutants of the green fluorescent protein (GFP) *Gene* **173** 33–8
[16] Bueno O F, Robinson L C, Alvarez-Hernandez X and Leidenheimer N J 1998 Functional characterization and visualization of a GABAA receptor-GFP chimera expressed in *Xenopus* oocytes *Mol. Brain. Res.* **59** 165–77
[17] Lu J, Daly C M, Parker M D, Gill H S, Piermarini P M, Pelletier M F and Boron W F 2006 Effect of human carbonic anhydrase II on the activity of the human electrogenic Na/HCO_3 cotransporter NBCe1-A in *Xenopus* oocytes *J. Biol. Chem.* **281** 19241–50
[18] Tanida I, Ueno T and Uchiyama Y 2014 A super-ecliptic, pHluorin-mKate2, tandem fluorescent protein-tagged human LC3 for the monitoring of mammalian autophagy *PLoS One* **9** e110600
[19] Visser A J, Westphal A H, Skakun V V and Borst J W 2016 GFP as potential cellular viscosimeter *Methods. Appl. Fluoresc.* **4** 035002
[20] Takahashi E, Takano T, Numata A, Hayashi N, Okano S, Nakajima O, Nomura Y and Sato M 2005 Genetic oxygen sensor, Conference Proceedings *Oxygen Transport to Tissue XXVI* (*Advances in Experimental Medicine and Biology* 556) (Berlin: Springer) pp 39–44
[21] Lakowicz J R, Szmacinski H, Nowaczyk K, Berndt K W and Johnson M 1992 Fluorescence lifetime imaging *Anal. Biochem.* **202** 316–30
[22] Berezin M Y and Achilefu S 2010 Fluorescence lifetime measurements and biological imaging *Chem. Rev.* **110** 2641–84
[23] Venkatachalan S P, Bushman J D, Mercado J L, Sancar F, Christopherson K R and Boileau A J 2007 Optimized expression vector for ion channel studies in *Xenopus* oocytes and mammalian cells using alfalfa mosaic virus *Pflügers Archiv-European Journal of Physiology* **454** 155–63
[24] Dönnes P and Höglund A 2004 Predicting protein subcellular localization: past, present, and future *Genomics Proteomics Bioinformatics* **2** 209–15
[25] Snapp E 2005 Design and use of fluorescent fusion proteins in cell biology *Curr. Protoc. Cell Biol.* **27** 4.1–4.13
[26] Campbell T N and Choy F Y 2001 The effect of pH on green fluorescent protein: a brief review *Mol. Biol. Today.* **2** 1–4
[27] Nakabayashi T, Wang H-P, Kinjo M and Ohta N 2008 Application of fluorescence lifetime imaging of enhanced green fluorescent protein to intracellular pH measurements *Photochemical & Photobiological Sciences* **7** 668–70
[28] Heikal A A, Hess S T and Webb W W 2001 Multiphoton molecular spectroscopy and excited-state dynamics of enhanced green fluorescent protein (EGFP): acid–base specificity *Chem. Phys.* **274** 37–55
[29] Bhagat A A S, Bow H, Hou H W, Tan S J, Han J and Lim C T 2010 Microfluidics for cell separation *Med. Biol. Eng. Comput.* **48** 999–1014
[30] Marchant J S and Parker I 2001 *Xenopus* tropicalis oocytes as an advantageous model system for the study of intracellular Ca(2+) signalling *Br. J. Pharmacol.* **132** 1396–410
[31] Li W, Houston K D and Houston J P 2017 Shifts in the fluorescence lifetime of EGFP during bacterial phagocytosis measured by phase-sensitive flow cytometry *Sci. Rep.* **7** 40341
[32] Borst J W, Hink M A, van Hoek A and Visser A J 2005 Effects of refractive index and viscosity on fluorescence and anisotropy decays of enhanced cyan and yellow fluorescent proteins *Journal of Fluorescence* **15** 153–60
[33] Suhling K, Siegel J, Phillips D, French P M W, Lévêque-Fort S, Webb S E D and Davis D M 2002 Imaging the environment of green fluorescent protein *Biophys. J.* **83** 3589–95
[34] Tregidgo C L, Levitt J A and Suhling K 2008 Effect of refractive index on the fluorescence lifetime of green fluorescent protein *J. Biomed. Opt.* **13** 8
[35] Van Manen H-J, Verkuijlen P, Wittendorp P, Subramaniam V, Van den Berg T K, Roos D and Otto C 2008 Refractive index sensing of green fluorescent proteins in living cells using fluorescence lifetime imaging microscopy *Biophys. J.* **94** L67–9
[36] Pliss A, Zhao L, Ohulchanskyy T Y, Qu J and Prasad P N 2012 Fluorescence lifetime of fluorescent proteins as an intracellular environment probe sensing the cell cycle progression *ACS Chem. Biol.* **7** 1385–92
[37] Ganguly S, Clayton A H and Chattopadhyay A 2011 Fixation alters fluorescence lifetime and anisotropy of cells expressing EYFP-tagged serotonin1A receptor *Biochem. Biophys. Res. Commun.* **405** 234–7
[38] Joosen L, Hink M A, Gadella TW Jr and Goedhart J 2014 Effect of fixation procedures on the fluorescence lifetimes of Aequorea victoria derived fluorescent proteins *J. Microsc.* **256** 166–76